PHYSICAL REVIEW E **74**, 030903(R) (2006)

Stochastic synchronization in finite size spiking networks

Brent Doiron,[1,2] John Rinzel,[1,2] and Alex Reyes[1]
[1]*Center for Neural Science, New York University, New York, New York 10003, USA*
[2]*Courant Institute of Mathematical Sciences, New York University, New York, New York 10003, USA*
(Received 18 December 2005; published 13 September 2006)

We study a stochastic synchronization of spiking activity in feedforward networks of integrate-and-fire model neurons. A stochastic mean field analysis shows that synchronization occurs only when the network size is sufficiently small. This gives evidence that the dynamics, and hence processing, of finite size populations can be drastically different from that observed in the infinite size limit. Our results agree with experimentally observed synchrony in cortical networks, and further strengthen the link between synchrony and propagation in cortical systems.

DOI: 10.1103/PhysRevE.74.030903 PACS number(s): 87.18.Sn, 05.40.−a, 05.45.Xt, 87.19.Bb

In vitro culture [1], slice [2], and *in vivo* [3] cortical networks suggest that cortical processing is performed by many interacting populations of neurons. Each population is finite in size and shows noninfinitesimal cell-cell interaction strengths [4,5]. As signals propagate through successive mesoscopic populations they modulate cortical dynamics on a macroscopic scale. Past theoretical studies have primarily focused on interactions between only one or two neural populations [5–11], where the consequence of the finite size of a population is merely to weakly perturb the dynamics predicted in the infinite size limit [6,7]. How spiking networks organize and transfer their activity across a large number of populations, each having a finite size, is yet unclear. We study this basic problem in networks of spiking neurons with feedforward architecture, commonly termed "synfire" chains [4] [see Fig. 1(a)].

It is well known that neurons deep in the chain of a feedforward assembly develop a synchronous spike discharge [12,13]. For illustration we show a network of *in vitro* cortical neurons whose activities were reconstructed using an iterative procedure [13]. Asynchronous input to the first population leads to synchronous activity in successive populations in the chain. A synchronous population response is expected at the start of the stimulus [<0.5 s in Fig. 1(b)], since all neurons share a common onset time. What is curious is the revival of synchrony after a seemingly random period of relative asynchrony [see the shaded part of Fig. 1(b)]. This *stochastic synchronization* (SS) is robust under a wide range of network configurations [12,13] and its function is hotly debated [14]. Despite the ubiquity and importance of SS, the underlying mechanisms and the key system parameters are not yet known.

We present an integrate-and-fire (IF) network that captures the essence of SS. A dynamic mean field analysis shows that in the limit of infinite system size we expect no synchronization beyond the transient response. A stochastic perturbation of the mean field equations, accounting for a finite but still large system size, is required to produce SS. Furthermore, the degree of SS scales inversely with network size. This strong dependence on system size for feedforward networks is quite surprising, and suggests that the number of neurons in networks may be a critical parameter for cortical processing.

We consider M populations of N neurons connected in a feedforward chain. Spiking dynamics are modeled using a linear IF neuron [10], where the membrane potential V_{im} of the ith neuron in population m obeys

$$\frac{dV_{im}}{dt} = -\beta + I_{im}(t). \tag{1}$$

Additionally, Eq. (1) includes a spike-reset rule: $V_{im}(t^+) = V_R$ whenever $V_{im}(t) = V_T$ with $V_R < V_T$. The spike time t_{ij} is the jth time this condition is met. We set a lower barrier at $V_L \leq V_R$ so that $V_{im} \geq V_L$. $I_{im}(t)$ is the sum of all inputs driving cell im at time t. An internal process, $\beta > 0$, forces V_{im} to V_L when $I_{im}(t) = 0$.

Neuron im receives C_{ex} excitatory and C_{in} inhibitory inputs from randomly chosen neurons in the population $m-1$. The ratios $C_{ex}/N = \epsilon_{ex}$ and $C_{in}/N = \epsilon_{in}$ are fixed to small values. When a presynaptic neuron $j(m-1)$ fires, neuron im receives an instantaneous kick of strength $\rho_{ijm} = J_{ex}/C_{ex}$ $(= J_{in}/C_{in})$ if there is an excitatory (inhibitory) input, else $\rho_{ijm} = 0$. Note that the kick strength scales as $1/N$. Each neuron also receives an independent stochastic forcing $I_{im,e}(t) = \sigma_e \eta_{im,e}(t)$ with $\langle \eta_{im,e}(t) \rangle = 0$ and $\langle \eta_{im,e}(t) \eta_{jm',e}(t') \rangle = \delta_{ij}\delta_{mm'}\delta(t-t')$ ($\langle \cdot \rangle$ is a temporal average). $I_{im,e}(t)$ models a balanced noisy external input that is independent of processing within the chain [12,13]. The total driving input to neuron im is then

$$I_{im}(t) = \sum_k \rho_{ijm} \sum_j \delta(t - t_{kj(m-1)}) + I_{im,e}(t), \tag{2}$$

where $t_{kj(m-1)}$ is the kth spike from neuron j in population $m-1$. The firing statistics of the input layer ($m=0$) are uncorrelated Poisson processes of rate $\nu_0 \Theta(t)$ with $\Theta(t)$ a Heaviside function.

Simulations of the IF network with $N=500$ and $M=10$ show randomly occurring epochs of synchrony in the deep populations long after the transient period [Fig. 1(c); note the time scale]. The SS is qualitatively similar to both experiments [Fig. 1(b)] and other simulations of feedforward systems [12,13].

A mean field treatment of the stochastic system Eqs. (1) and (2) is computed in the diffusion limit [5,6]. Specifically, $I_{im}(t)$ is determined by the firing probability of population

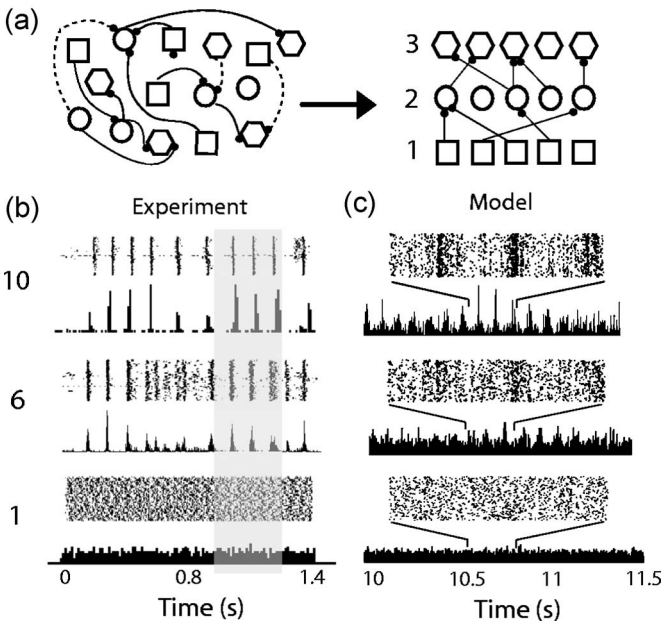

FIG. 1. SS in experimental and model feedforward networks. (a) Schematic of the "unfolding" of a feedforward architecture from a seemingly undirected network of neurons. We neglect feedback and interpopulation coupling (dashed lines). (b) Spike-time rasters (dots) and population activity histograms (solid; bin width 1 ms) from iteratively constructed *in vitro* networks of cortical neurons (200 neurons per population); see [13] for details. No external noise was delivered to the neurons. As shown previously [13], adding noise to the *in vitro* network did not prevent synchrony. (c) Simulations of a feedforward network with linear IF neurons. We show network behavior 10 s after stimulus onset, long after onset-induced synchrony has dissipated. Unlike in experiments, external noise was added (see text). Dot rasters are shown for a portion of the histogram. Model parameters are $N=500, \beta=0.5, J_{ex}=2, J_{in}=-0.96, V_T=1, V_L=V_R=0, \sigma_e=0.31$, $\epsilon_{ex}=0.1$, and $\epsilon_{in}=0.048$. Simulations were performed with a stochastic Euler scheme with a time step of 10^{-5} [15]. In both panels (b) and (c) we show only populations 1, 6, and 10 [left-hand side of (b)].

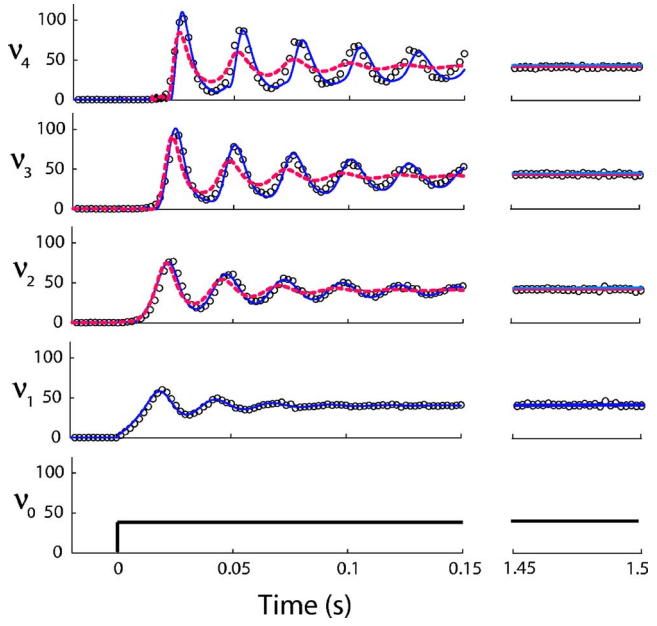

FIG. 2. (Color online) DMFT predicts only transient synchrony. Expected firing rate $\nu_m(t)$ for $m=0,\ldots,4$ with $F_m(t)=0$. Open circles are simulations of the IF network, lines are simulations of the mean field with either $R_{m,eq}$ defined appropriately [18] (solid blue lines), or $R_{m,eq}=1$ (dashed red lines). The right panels show the solutions long after the initial transient. Model parameters are the same as in Fig. 1(c) except $\nu_0=40$ Hz, $\sigma_e=0.63$, and $N=1000$.

$m-1$, $\nu_{m-1}(t)=(1/N)\Sigma_{i,j}\delta(t-t_{ij(m-1)})$. Despite the Poisson input to the chain ($m=0$) the spike trains from neurons deeper in the chain are non-Poisson [17], in which case in the diffusion limit $I_{im}(t)$ is a colored noise process [16,17]. This complicates a mean field analysis by adding extra state variables to the field equations [17].

Fortunately, for nonleaky IF systems the population response to a simple colored process is well approximated by the response to a rescaled white noise process [16]. Consequently, the diffusion limit can be described as

$$I_{im}(t) \approx \mu_m(t) + \sigma_m(t)\xi_{im}(t),$$

$$\mu_m(t) = [J_{ex} + J_{in}]\nu_{m-1}(t),$$

$$\sigma_m^2(t) = [J_{ex}^2/C_{ex} + J_{in}^2/C_{in}]R_{m-1,eq}^2\nu_{m-1}(t) + \sigma_e^2, \qquad (3)$$

where $\langle\xi_{i,m}(t)\rangle=0$ and $\langle\xi_{i,m}(t)\xi_{j,m}(t')\rangle=\delta_{ij}\delta(t-t')$. Here we have scaled $\sigma_m^2(t)$ by the coefficient of variation of the interspike interval distribution of population $m-1$ labeled $R_{m,eq}$ (computed for $t\to\infty$). While this rescaling is exact in equilibrium [16], we conjecture that it applies to nonequilibrium statistics as well. We note that for $\epsilon_{ex}, \epsilon_{in} \ll 1$ any shared fluctuations can be neglected [6].

The stochastic IF network given by Eqs. (1) and (3) is described by a sequence of Fokker-Planck equations [15], one for each population density $P_m(V,t)$:

$$\partial_t P_m(V,t) = \mathcal{L}_m P_m(V,t) + \nu_m(t)\delta(V-V_R),$$

$$\mathcal{L}_m = \partial_V\{-\mu_m(t) + [\sigma_m(t)^2/2]\partial_V\},$$

$$\nu_m(t) = -[\sigma_m^2(t)/2]\partial_V P_m(V,t)\big|_{V=V_T}. \qquad (4)$$

Solutions to Eq. (4) are constrained by the boundary conditions $P_m(V_T,t)=0$ and $\{\mu_m(t)-[\sigma_2^2(t)/2]\partial/\partial V\}P_m(V,t)|_{V=V_L}=0$, along with a proper normalization $\int_{V_L}^{V_T}P_m(V,t)dV=1$. In Eq. (4) we set $\mu_m-\beta\to\mu_m$. We express $P_m(V,t)$ in terms of a dynamic basis set (see [9] for a review and [7] for the specific application to linear IF models).

Briefly, we use a complete basis set of eigenfunctions $\{\psi_{q,m},\phi_{q,m}\}$, where $\phi_{q,m}(V)$ and $\psi_{q,m}(V)$ are the respective left and right eigenvectors associated with eigenvalue $\lambda_{q,m}$ of $\mathcal{L}_m$. We expand $P_m(V,t)=\Sigma_{q=-\infty}^{\infty}a_{q,m}(t)\phi_{q,m}(V)$, where $a_{q,m}=(\psi_{q,m},P_m)$ with $(f,g)=\int_{V_R}^{V_T}f(V)g(V)dV$. It can be shown [7,9] that the vector $\vec{a}_m=[a_1,a_{-1},a_2,\ldots]^T$ obeys the following sequence of nonlinear differential equations:

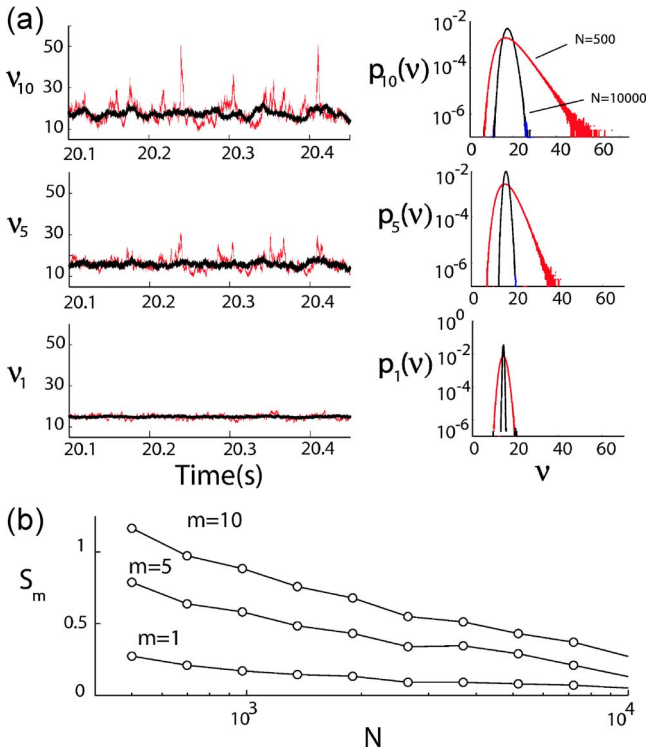

FIG. 3. (Color online) SS obtained in the finite size mean field equations. (a) Realizations of the SMFT for $N=500$ (thin red) and 10 000 (thick black) for $m=1,5$, and 10 (left). Estimated distributions $p_m(\nu)$ (right). (b) Skewness S_m for varying N and m computed from simulations of the IF network. Model parameters are the same as in Fig. 1(c) but with $\sigma_e=0.54$ and $\nu_0=15$ Hz.

$$d\vec{a}_m/dt = [\mathbf{\Lambda} + [d\nu_{m-1}/dt]\mathbf{C}_m]\vec{a}_m + (d\nu_{m-1}/dt)\vec{c}_m + F_m(t)\zeta_m(t)\vec{\psi}(V_R),$$

$$\nu_m(t) = \Phi_{m,eq}(\mu_m,\sigma_m) + \vec{f}_m\cdot\vec{a} + F_m(t)\zeta_m(t). \quad (5)$$

$\mathbf{\Lambda}$ is a diagonal matrix of the eigenvalues of $\mathcal{L}_m$ [7]. The nonequilibrium mode interaction matrix $\mathbf{C}_m$ has elements $c_{ij,m}=(\partial_{\nu_{m-1}}\psi_{i,m},\phi_{j,m})$, the equilibrium to nonequilibrium mode vector $\vec{c}_m$ has elements $c_{i,m}=(\partial_{\nu_{m-1}}\psi_{i,m},\phi_{0,m})$, and the eigenmodes at threshold are given by the vector $\vec{f}_m$ with elements $f_q=-[\sigma^2(t)/2]\partial_V\phi_q(V)|_{V=V_T}$. $\Phi_{m,eq}(t)$ is the equilibrium transfer function of population m [18]. In practice we consider only a finite number of modes ($n=6$).

$\nu_m(t)$ [as given by Eqs. (3) and (4)] is exact in the limit $N\to\infty$. To correct for the case when $N<\infty$ we use a previously proposed scheme [6–8] to perturb $\nu_m(t)$ and $\vec{a}_m$ with a Gaussian white noise term $\zeta_m(t)$ of intensity $F_m(t)=\sqrt{\nu_m(t)/N}$ [properly scaled by the $\vec{\psi}_m(V_R)$ for $\vec{a}_m$]. The correction term models the inaccuracies in the Fokker-Planck equation in describing the firing probability for a finite ensemble of neurons.The mean field is now a sequence of stochastic partial differential equations.

In what follows we will compare the dynamics of a deterministic mean field theory (DMFT), where we naively take $F_m(t)=0$, to that of the stochastic mean field theory (SMFT) where we account for $N<\infty$. Specifically, the DMFT computes $\nu_m(t)$ as an average over V_{im}, ρ_{ikm}, the processes given by ν_0, and $I_{im,e}$, whereas the SFMT treats $\nu_m(t)$ as an average only over V_{im}.

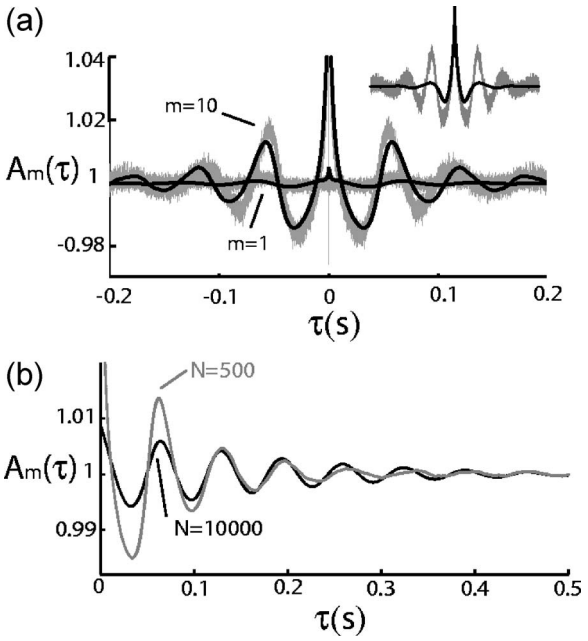

FIG. 4. Oscillations accompany SS. (a) Normalized autocorrelations $A_1(\tau)$ and $A_{10}(\tau)$ calculated for simulations of the IF network (gray) and the SMFT (black) when $N=500$. Inset: $A_{10}(\tau)$ computed with $R_{m,eq}=1$ (black) superimposed with the result from IF simulations (gray). (b) $A_{10}(\tau)$ computed with $N=500$ and 10 000. Parameters are identical to those of Fig. 3.

Finally, the basis set $\{\psi_{q,m},\phi_{q,m}\}$, as well as $\mathbf{\Lambda}_m$, $\mathbf{C}_m$, $\vec{c}_m$, and $\vec{f}_m$ inherit the time dependence of $\nu_{m-1}(t)$. Since our focus is on large-amplitude fluctuations of $\nu_m(t)$, as opposed to small fluctuations computable with a linear response [7,11], we solve Eqs. (3) and (5) by computing the eigensystem at a discrete set of input rates $\{\nu_{k,m}\}_k$ with $\nu_{k+1,m}-\nu_{k,m}=\Delta\nu$. The eigensystem for $\nu_{k,m}\le\nu_m(t)\le\nu_{k+1,m}$ is computed as a linear interpolation between the eigensystems defined by $\nu_{k,m}$ and $\nu_{k+1,m}$. Accurate results were obtained with $\Delta\nu=0.5$.

We compare simulations of the IF network Eqs. (1) and (2) and numerical solutions of the DMFT in Eqs. (3) and (5) for $m=0$ to $m=4$ (Fig. 2). Comparing conditions where the diffusive term is rescaled by the appropriate $R^2_{m,eq}$ (solid blue line) [18], and where we force $R_{m,eq}=1$ (dashed red line) shows that only the rescaled diffusion system accurately describes the transient response of the IF network in the deeper populations. Despite the success of the rescaled DMFT in describing the transient dynamics, all solutions eventually decay to an asynchronous state (right panels in Fig. 2). This behavior is distinct from the SS observed in both the finite size experiments and IF networks [Figs. 1(b) and 1(c)].

In contrast to the DMFT the SMFT accurately replicates SS. $\nu_{10}(t)$ computed using SMFT with $N=500$ shows brief epochs of high firing probability, representing randomly

timed epochs of SS [Fig. 3(a), thin red lines]. These epochs are absent in superficial populations and in all populations with $N=10\,000$ [Fig. 3(a), thick black lines]. The estimated distributions of firing probability $p_m(\nu)$ when $N=500$ are distinctly asymmetric for large m, with the long tails arising from the synchronous epochs [Fig 3(a), right panels]. To quantify we compute the skewness $S_m=\kappa_{3,m}/\kappa_{2,m}^{3/2}$ of the distributions $p_m(\nu)$ for different values of N and m where $\kappa_{n,m}=\int[\nu_m(t)-\langle\nu_m(t)\rangle]^n p_m(\nu)d\nu$ [Fig. 3(b)]. S_m clearly increases with m, particularly when N is small. Intuitively, the growth of S_m with m depends on a combination of the nonlinear amplification of transient activity in the feedforward network, and the finite size perturbations.

To further quantify SS obtained with the SMFT we compute the normalized autocorrelation $A_m(\tau)=\langle\nu_m(t)\nu_m(t+\tau)\rangle/\langle\nu_m(t)\rangle^2$ [Fig. 4(a)]. With $N=500$, there is an excellent agreement of $A_1(\tau)$ and $A_{10}(\tau)$ for simulations of the IF network and the SMFT. Interestingly, there is a distinct stochastic oscillation in $\nu_{10}(t)$, with a frequency that is roughly $\langle\nu_m(t)\rangle\approx\Phi_{m,eq}$. This frequency is directly related to the eigenspectrum of $\mathcal{L}_m$. $A_m(\tau)$ computed from the SMFT with the Poisson assumption are not oscillatory, unlike the IF simulations (see inset). Figure 4(b) compares $A_{10}(\tau)$ for $N=500$ and 10 000. For small $|\tau|$ the oscillatory nature of the small network is more prominent than for a large network. However, for larger $|\tau|$ both large and small networks have similar coherence, indicating synchrony to be truly a stochastic phenomenon with finite memory. For $N<250$ the theory applies only qualitatively to the network simulations.

In summary, we have provided a simple, mechanism for SS in a network of spiking neurons. The synchrony arises from a combination of finite-size-induced perturbations of network activity [6,7], and amplification of activity through successive populations [12]. A SMFT shows how finite-size-induced fluctuations in superficial populations (order $1/\sqrt{N}$) are compounded and become large amplitude (order 1) epochs of damped oscillatory synchrony in deeper populations. We remark that for $N=500$ the amplitudes of synaptic inputs are more comparable to those experimentally measured $[J_{expt}/C_{expt}, J_{in}/C_{in}\approx(V_T-V_F)/25]$ than for $N=10\,000$ [13]. Our results are consistent with the experimental results shown in Fig. 1(b) and [13], and the synchronous activity observed in both spontaneous and evoked cortical activity [1,3]. Further, our study shows how interactions of multiple populations of spiking neurons can be critically dependent on system size. A crucial next step is determining how stochastic synchronization interacts with stimulus-induced dynamics to determine cortical responses.

We thank H. Câteau, J. del la Rocha, E. Shea-Brown, and M. Mattia for useful discussions. This research was funded by HSFP-LT788 (B.D), NIH MH-62595 (J.R), and NIH DC005787 (A.R).

[1] R. Segev *et al.*, Phys. Rev. Lett. **88**, 118102 (2002); J. M. Beggs and D. Plenz, J. Neurosci. **23**, 11167 (2003).
[2] Y. Ikegaya *et al.*, Science **304**, 559 (2004).
[3] M. Tsodyks *et al.*, Science **286**, 1943 (1999).
[4] M. Abeles, *Corticonics: Neural Circuits of the Cerebral Cortex* (Cambridge University Press, Cambridge, U.K., 1991).
[5] W. Gerstner and W. M. Kistler, *Spiking Neuron Models* (Cambridge University Press, New York, 2002).
[6] N. Brunel and V. Hakim, Neural Comput. **11**, 1621 (1999).
[7] M. Mattia and P. Del Giudice, Phys. Rev. E **66**, 051917 (2002); **70**, 052903 (2004).
[8] N. Hohn and A. N. Burkitt, Phys. Rev. E **63**, 031902 (2001).
[9] B. W. Knight, Neural Comput. **12**, 473 (2000).
[10] S. Fusi and M. Mattia, Neural Comput. **11**, 633 (1999).
[11] B. W. Knight, J. Gen. Physiol. **59**, 734 (1972); M. Spiridon and W. Gerstner, Network **10**, 257 (1999); N. Brunel *et al.*, Phys. Rev. Lett. **86**, 2186 (2001); B. Lindner *et al.*, Phys. Rev. E **66**, 031916 (2002).
[12] M. Diesmann *et al.*, Nature (London) **402**, 529 (1999); H. Câteau and T. Fukai, Neural Networks **14**, 675 (2001); H. Hasegawa, Phys. Rev. E **67**, 041903 (2003); V. Litvak *et al.*, J. Neurosci. **23**, 3006 (2003); S. Wang *et al.*, Phys. Rev. Lett. **96**, 018103 (2006); M. C. van Rossum *et al.*, J. Neurosci. **22**, 1956 (2002); N. Masuda and K. Aihara, Phys. Rev. Lett. **88**, 248101 (2002).
[13] A. Reyes, Nat. Neurosci. **6**, 593 (2003).
[14] M. Abeles, Science **304**, 523 (2004); M. N. Shadlen and W. T. Newsome, J. Neurosci. **18**, 3870 (1998).
[15] H. Risken, *The Fokker-Planck Equation*, 2nd ed. (Springer-Verlag, Berlin, 1989).
[16] R. Moreno, Phys. Rev. Lett. **89**, 288101 (2002).
[17] H. Câteau and A. D. Reyes Phys. Rev. Lett. **96**, 058101 (2006).
[18] The linear IF model has a simple first passage time relation [10] with $\Phi_m=\{[V_T/\mu_m(t)z](z-1+e^{-z})\}^{-1}$ and $R_{m,eq}=\lim_{t\to\infty}\sqrt{e^{-2z}+4e^{-z}(z+1)+2z-5}/(e^{-z}+z-1)$ where $z=2\mu_m(t)V_T/\sigma_m^2(t)$.